

**THIS IS THE PEER REVIEWED VERSION OF
THE FOLLOWING ARTICLE:**

Felice De Santis, Roberto Pantani

“DEVELOPMENT OF A RAPID SURFACE TEMPERATURE VARIATION SYSTEM AND APPLICATION TO MICRO-
INJECTION MOLDING”

Journal of Materials Processing Technology

Volume 237, 1 November 2016, Pages 1-11

DOI: 10.1016/j.jmatprotec.2016.05.023

WHICH HAS BEEN PUBLISHED IN FINAL FORM AT

<https://linkinghub.elsevier.com/retrieve/pii/S0924013616301649>

THIS ARTICLE MAY BE USED ONLY FOR NON-COMMERCIAL PURPOSES

Development of a rapid surface temperature variation system and application to micro-injection molding

Felice De Santis*, Roberto Pantani

Department of Industrial Engineering, University of Salerno - Via Giovanni Paolo II, 132, 84084 Fisciano (SA), Italy

*Corresponding Author at:

Department of Industrial Engineering, University of Salerno

Via Giovanni Paolo II, 132, 84084 Fisciano (SA), Italy

Tel: +39 089 96 4013

Email address: fedesantis@unisa.it

ABSTRACT: In conventional injection molding, the mold temperature control is obtained by a continuous cooling method, in which a coolant with constant temperature is circulated in the cooling channels to cool the mold and the polymer melt. During the filling stage, this causes an abrupt polymer solidification close to the mold surface, which reduces the section open to flow and, due to the viscosity increase, causes a decrease of the ability of the polymer melt to fill the cavity. This issue is particularly significant for micro-injected parts in which high aspect ratios are precluded because of premature solidification. In this work, a system for rapid surface temperature control was designed, built and applied to a cavity for micro-injection molding. The system consists in an electrical resistive thin component and an insulation layer and can increase the mold surface temperature of some tenths of a degree Celsius in a time of the order of one second. The system is versatile enough to allow the control of thermal histories during the whole process and at different positions inside the cavity. Injection molding tests were then carried out with this system by using a general purpose isotactic polypropylene and a cavity 200 μm thick in order to check the effect of surface heating on reachable flow length and morphology of the molded parts. The effect of mold temperature on the flow length was as expected dramatic on both the flow length and the obtained morphology: the samples molded with a high mold temperature presented a spherulitic morphology in the whole cross-section, while with a low surface temperature the spherulitic morphology was detectable only at the positions close to the midplane whereas the layer closer to the surface present a very oriented structure due to flow taking place at low temperature.

Keywords: Micro-injection molding; Rapid heat cycle molding; Thermoplastic materials; Mold design.

1. Introduction

Micro-injection molding is a technology for high value added products of increasing application in the areas of medical technology, as components of optical systems, as micro parts in microfluidics, biotechnology, and electronics (Giboz et al., 2007). Although the concept of micro-part has many interpretations, Whiteside et al. (Whiteside et al., 2004)

consider that, depending on the areas of interest, a micro part should present one of the following three characteristics:

- a weight of a few milligrams
- features with dimensions in the micrometer scale
- tolerances in the micrometer scale

The reduction of part dimensions introduces additional issues with respect to conventional injection molding, together with the advantage of the most efficient process for the large-scale production. The cavity thickness is the decisive parameter to the molding of small parts as reported by Song et al. (Song et al., 2007).

The control of mold temperature is important in the injection molding process, and a crucial feature for micro parts. Ideally, the temperature should be higher than solidification point during filling, in order to allow a complete filling without an excessive pressure and stress on the material; after filling, the temperature should quickly decrease below the solidification point to obtain a solid polymeric part in reasonable times (Jansen and Flaman, 1994). Therefore, a high temperature during filling has been reported to improve the surface appearance (Zhao et al., 2011), to reduce the weld lines (Wang et al., 2013) and to increase the replication quality (Meister et al., 2015). The control of cooling rate after filling is also critical for the morphology (e.g., degree of crystallinity or orientations as reported by Liparoti et al. (Liparoti et al., 2015)) and thus mechanical properties (e.g. tensile strength as reported by Pantani et al. (Pantani et al., 2005)). The surface quality in replicating micro-features is one of the most important process characteristics and constitutes a manufacturing constraint in applying injection molding in a range of micro-engineering applications (Sha et al., 2007). In particular Lucchetta et al. (Lucchetta et al., 2012) developed a technology for rapid heating and cooling of injection molds to analyze the effect of fast variations of the mold temperature on the improvement of micro features replication and moldings appearance.

Despite the huge literature dedicated to the effect of mold temperature on standard injected molded samples, only limited attention was devoted to the micro-injection molding. Attia and Alcock (Attia and Alcock, 2010) investigated the developments that have been achieved in different aspects of micro-injection molding of microfluidic devices. Further attempts have been made to meet this objective and reviews of the methods can be found in the literature. Yao et al. (Yao et al., 2008) offer a constructive overview on the state of the art in mold rapid heating and cooling, with the goal of explaining the working mechanisms and providing unbiased accounts of the pros and cons of existing processes and techniques. Among the several possibilities, the so-called “coating heating”, namely the possibility of heating just

the surface of the mold by means of thin electrical resistances, presents many advantages: the optimal use of heating power (since just the needed part of the mold is heated) and the possibility of a temperature control. The rapidity of the temperature evolution is obviously crucial, as recently indicated by Berger et al. (Berger et al., 2014). To overcome the difficulties to fill a thin-wall cavity with long flow paths also special resins (e.g. DSM Akulon Ultraflow polyamide 6) with high flow properties were developed.

In this work, a novel system for controlling the surface temperature of a mold for micro-injection molding has been developed to overcome the limitations of the available technologies and it has been used to analyze the effect of fast variations of the mold temperature to the injection molding of a polypropylene in a 200 μm thick cavity.

The potential processing benefits of the proposed system go from increased productivity (cycle time reduction) to increased freedom of design (flow improvement), as well as increased quality levels (surface appearance, weldability) in the finished part.

2. Experimental Section

2.1. Design and realization of the mold

The injection molding machine adopted in this work is a HAAKE Minijet II by Thermo Scientific. This machine is a mini-injection molding system, that adopts a pneumatic piston to control the pressure during the molding. The molds for HAAKE Minijet II present a truncated cone shape, with a diameter which changes from 50 mm (at the gate side) to 35 mm over a length of about 90 mm.

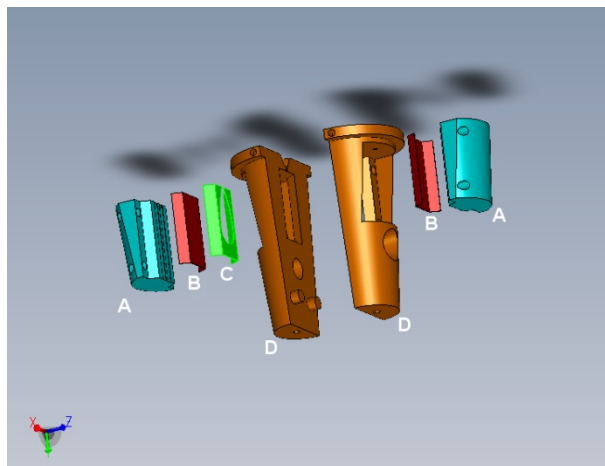


Fig. 1. Exploded view drawing of the elements composing the mold. A: inserts; B: heated slabs; C: cavity; D: main mold halves.

Starting from the standard truncated cone shape of the molds used with HAAKE Minijet II, a novel system consisting in a mold with inserts and heating elements was designed, as shown in the exploded view drawing in Fig. 1, and carried

out. The implemented heating structure is based on very thin wire resistances, sealed in a carrier medium composed of polyimide film, each of them having the following characteristics: $R=120\ \Omega$, length=3.8 mm, width=5.0 mm, thickness=50 μm (volume, $V_R=0.95\ \text{mm}^3$). These heating resistances were positioned in a 5×2 matrix, as shown in the right part of Fig. 2, in order to cover a rectangular surface next to the cavity covering a surface about 8 mm wide and 20 mm long, and fixed on a steel slab 200 μm thick, as shown on the left part of Fig. 2. The thickness of the steel slab, which will constitute the cavity surface, was chosen in order to impart mechanical resistance and at the same time to allow for a fast heating and cooling. All the wire resistances, on both sides of the molds, were connected in parallel to the same voltage of the power supply. Two heated slabs (one for each side of the cavity) were built as described above. These slabs are identified by the letter B in Fig. 1.

Following the indication in the paper of Jansen and Flaman (Jansen and Flaman, 1994), a thin-insulation layer is used to separate the resistance layer from the mold. A PolyEtherSulfone (PES) film, 200 μm thick, was placed to separate the resistances from the mold, in between mold insert and heated slab shown as A and B in Fig. 1, respectively. PES was chosen because of its relatively low conductivity ($k_{PES}=0.15\ \text{W/m K}$) and above all high thermal stability, since it presents a heat-deflection temperature higher than 200°C.

Several geometries of the cavity were created in an additional steel slab (identified by letter C in Fig. 1), 200 μm thick, and a tapered gate with width 2.5 mm. This system allowed to change the cavity geometry quite easily. For all the tests shown in this work, the cavity has a rectangular shape, with width 5 mm and length 20 mm.

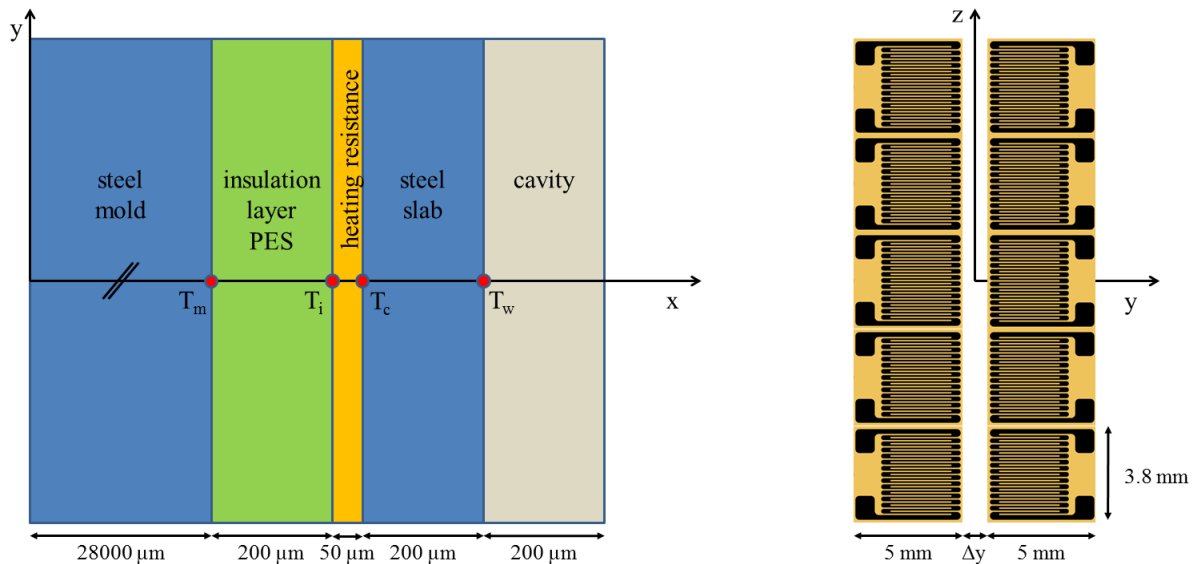


Fig. 2. Schematic of the layers on the left, with specific position for calculated temperatures: T_m between mold and insulation layer, T_i between insulation layer and heating resistances, T_c between heating resistances and steel slab, and T_w between steel slab and the cavity. Schematic of the heating resistances 5×2 matrix on the right.

Two steel inserts (identified by letter A in Fig. 1) were finally built to close the system and allow for the wires to come out from the mold. The inserts were built to host steel slabs with different thickness, and thus both the heated slabs and the cavity thickness could be changed. Furthermore it is easily understood that the heating system is modular and flexible, thus it can easily be adapted to whatever mold.

During mold design several simulations of the heating system were realized to verify potentials and troubles. In that analysis the system was approximated as consisting in 4 different elements in perfect contact (as shown in Fig. 2: polymer in the cavity, steel slab, heating resistances, insulation layer, mold insert), each with their physical properties and dimensions reported above. Simulation were performed solving time-dependent heat transfer partial differential equations using FlexPDE, a finite element commercial software, for the domain shown in Fig. 2.

In particular, the heat equation is a parabolic partial differential equation that describes the distribution of heat (or variation in temperature) in a given region over time.

For a function $T(x,y,t)$ of two spatial variables (x,y) , in Cartesian coordinates, and the time variable t , the heat equation for each element i is

$$\frac{k_i}{\alpha_i} \frac{\partial T}{\partial t} = \nabla \cdot (k_i \nabla T) + G_i \quad (1)$$

with continuity of temperature T and heat flux, $k_i \frac{\partial T}{\partial x}$ at the interface between each element, while the physical properties of each element, thermal conductivity k_i and thermal diffusivity α_i , and heat source term G_i are summarized in Table 1.

The temperature evolution is calculated with uniform initial temperature $T_0=27^\circ\text{C}$:

$$IC: t = 0, \forall (x, y) \quad T = T_0 \quad (2)$$

and with Neumann boundary conditions at the boundaries

$$\begin{aligned} BC1: x = 0, -k_{steel} (\nabla T \cdot \hat{n}) &= k_{steel} \frac{\partial T}{\partial x} = h(T_0 - T) \\ BC2: x = L, -k_{steel} (\nabla T \cdot \hat{n}) &= -k_{steel} \frac{\partial T}{\partial x} = h(T_0 - T) \\ BC3, BC4: y = \pm \frac{W}{2}, \frac{\partial T}{\partial y} &= 0 \end{aligned} \quad (3)$$

where the convective heat transfer coefficient for still air is assumed to be $h=5 \text{ W/m}^2 \text{ K}$.

The thickness of each element is also reported in Table 1, so that the total length in x -direction, L , is the sum of all of them, while the length in y -direction, W , is $54400 \mu\text{m}$ for all the elements.

Table 1 Physical properties of elements in the mold.

	x , thickness [μm]	α [m^2/s]	k [$\text{W}/\text{m K}$]	G [W/m^3]
steel, mold	28000	8.0×10^{-6}	15	0

PES, insulating layer	200	1.5×10^{-7}	0.15	0
heating resistances	50	2.0×10^{-7}	0.37	$P \times G_{hr}(t)$
steel, slab	200	8.0×10^{-6}	15	0

Finally the internal heat generation, due to joule heating P , and the control function G_{hr} are given by

$$P = \frac{V^2}{R} \frac{1}{V_R} \quad (4)$$

$$G_{hr}(t) = \begin{cases} 1 & \text{if } T_w < T_{sp} \text{ and } 0 \leq t \leq t_{hr} \\ 0 & \text{if } T_w > T_{sp} \text{ or } t > t_{hr} \end{cases} \quad (5)$$

Where V , R , and V_R are the applied voltage, the heating resistance (120 Ω), and the volume of the heating resistance (0.95 mm³), respectively.

As reported in Eq. 5, a simple temperature protocol is implemented: during the first part, that lasts t_{hr} , the temperature of the surface of the cavity, T_w , after thermal transient from T_0 , is kept at the set point temperature T_{sp} switching on and off the heating resistances. After t_{hr} , intended as the time to fill the cavity, the heating resistances are switched off performing a ballistic cooling of the mold, and in particular the cavity. Obviously more complicated temperature protocols could be designed and implemented too.

The principal parameters (time t_{hr} , the set point temperature T_{sp} , and the applied voltage V) are changed in the simulations to explore the potentialities of the designed system.

First of all, the simulation code was used with time $t_{hr}=30$ s, power supply $V=16$ V, the set point temperature $T_{sp}=120^\circ\text{C}$ and the resulting temperatures in specific positions are shown in left plot in Fig. 3. Obviously in the simulations these parameters could be easily changed, but without forgetting the thermal-mechanical properties of some of these elements (i.e. heating resistances can break exceeding some value of the applied voltage, PES layer can melt exceeding some value of the temperature).

One critical parameter is the distance (Δy in Fig. 2) between the heating resistances in the 5×2 matrix. Simulations of the system revealed that a distance of 0.5 mm is small enough to allow a homogeneous surface heating, as shown in the right plot of Fig. 3 and in Fig. 4.

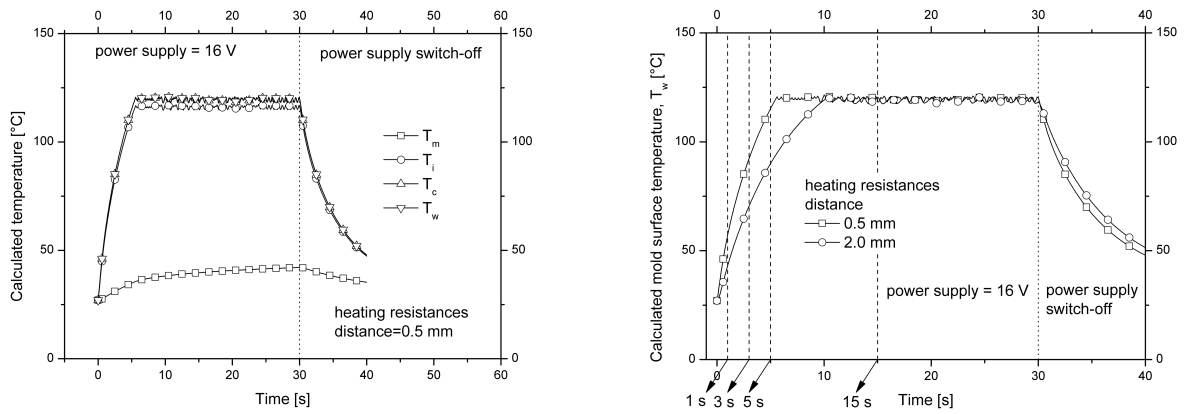


Fig. 3. Effect of the heating resistances distance on the temperature profile. Left: calculated temperature evolution at different position along x -direction, at $z,y=0$, with $\Delta y=0.5$ mm; right: calculated mold surface temperature evolution (T_w), at $z,y=0$, with distances of $\Delta y=0.5$ mm and 2.0 mm.

The results reported in Fig. 3 were useful to decide the position of the thermocouple. Indeed, it can be noticed that the temperature T_c at the interface between the heating elements and the steel slab is very close to the mold surface temperature. The thermocouple must thus be placed at that position T_c : at 7 mm from the gate (z direction in Fig. 2).

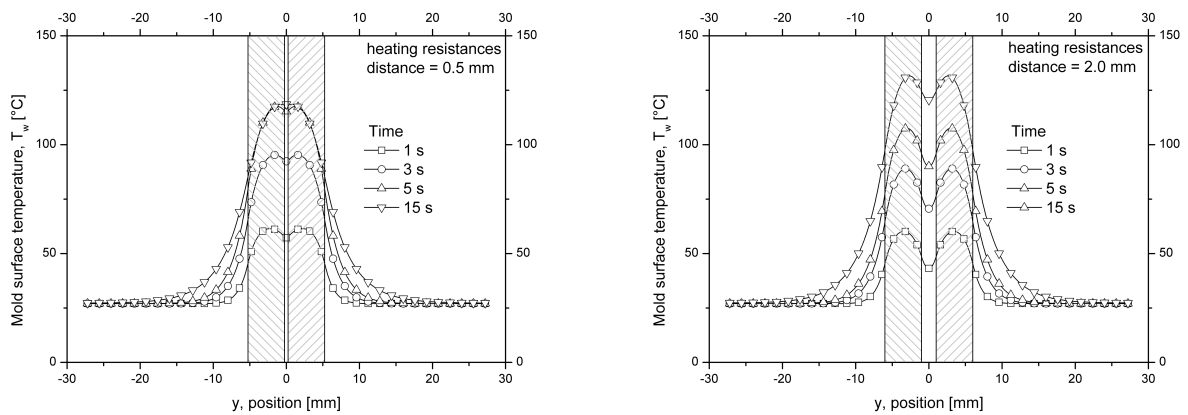


Fig. 4. Effect of the heating resistances distance on the temperature profile, on the left plot for distance of 0.5 mm and on the right plot for distance 2.0 mm. Heating resistances positions are reported as diagonal patterns.

Calculated mold surface temperature is more uniform with a distance of 0.5 mm of heating resistances, having each one a width of 5 mm in the y -direction, than the one with a distance of 2.0 mm, as shown in Fig. 4. Furthermore the surface of the cavity is 5 mm width so that this experiences an almost constant temperature profile evolution during heating and, more important, during constant temperature as shown after 5 s and 15 s with a distance of 0.5 mm of heating resistances.

2.2. Mold testing

The temperature is measured by using a thin wire thermocouple (Type T, 100 μm of diameter supplied by Omega Engineering ltd.) which is positioned at the very center of the heated surface, as near as possible to cavity surface, between the steel slab and heating resistances. A data acquisition board (DAQ NI-USB 6210 supplied by the National Instruments) is used to acquire the thermocouple measurements. A dedicated software was developed to provide the control of the temperature evolution in the ad-hoc device controlling the power supply to modulate the thermal history of the mold. This allowed to control the evolution of mold temperature and thus to impose a given heating and cooling rate (in the limit of the maximum values determined by the heating power and the cooling without power supply). Several experimental tests were conducted on the heated mold in order to verify its capabilities. The results of the first test are shown in Fig. 5, in which the applied voltage, and as a consequence the heating power, is changed. The maximum temperature was set to 120°C, which is high enough to induce a significant effect on polypropylene. In principle, the system can reach even higher temperatures, being limited to the melting temperature of PES which is higher than 200°C. After the system reaches the set point temperature value, the developed software keeps this temperature until the maximum heating time t_h of 30 s was reached. The highest applied voltage was 16 V, because the resulting current could break the heating resistances with higher voltage.

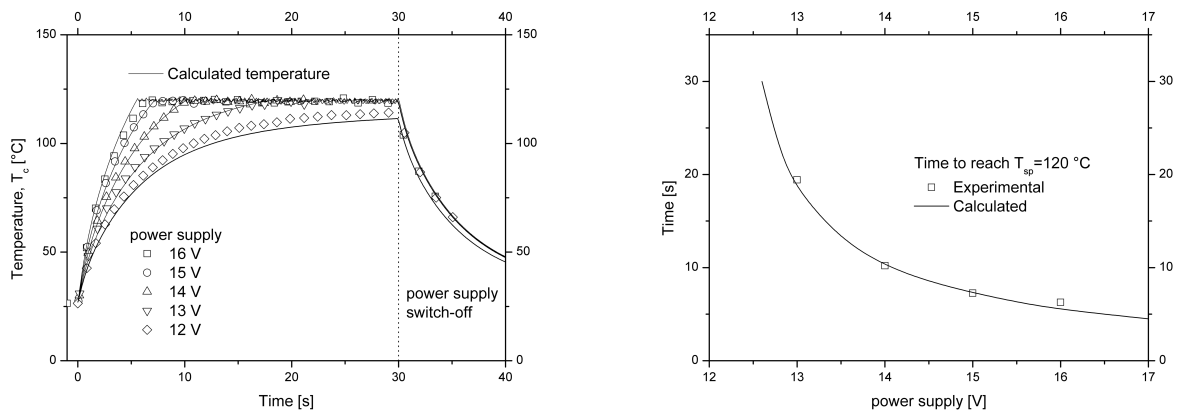


Fig. 5. On the left plot, the effect of the applied voltage on the temperature evolution: the experimental temperature (open symbols) is reported with corresponding simulated temperature (lines). On the right plot, the time needed to reach set point temperature, 120°C, is reported as function of the applied voltage.

The heating rate obviously decreases on decreasing the applied voltage, because for the same electrical resistance the current changes according Ohm law. For the lowest applied voltage the set point temperature could not be reached in 30 s. From the experimental temperature evolution reported in the left plot in Fig. 5 is possible to evaluate the heating

and cooling rates. This temperature change, $\frac{\partial T_c}{\partial t}$, is reported in Fig. 6 for the highest applied voltage ($V=16$ V): the

heating rate was about 20 K/s for the first 4 s, and the temperature of 120°C was reached after about 6 s.

The cooling rate after switching off the power supply was in the range 5-10 K/s, so that in 15 s the mold temperature is again below 40°C. It is worth mentioning that in its current configuration, the mold does not present any cooling system (ballistic cooling).

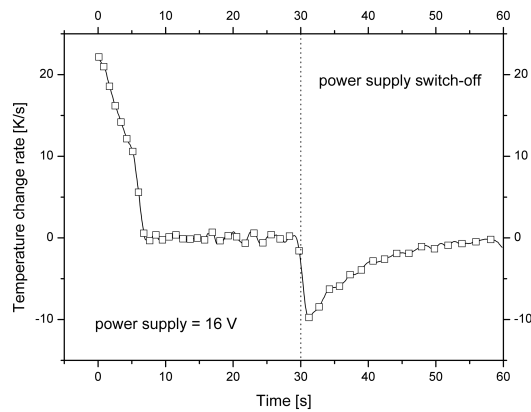


Fig. 6. Temperature change rate during a heating with a power supply of 16 V. The set point temperature is 120 °C, and power switch-off after 30 s.

Obviously, the possibility of controlling the temperature profile provides several opportunities. For instance, in Fig. 7 tests conducted by changing the set point temperature (the applied voltage was 16 V) are reported.

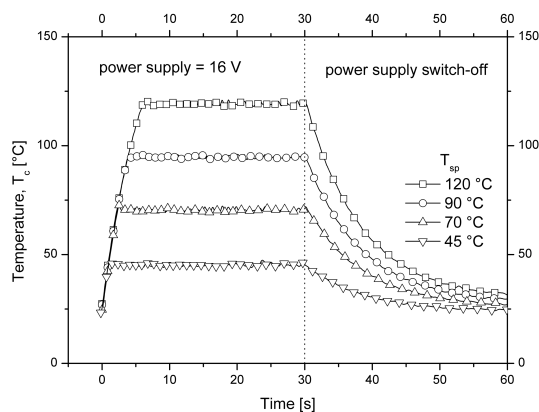


Fig. 7. Examples of maximum temperature control during a heating with a power supply of 16 V.

Furthermore, the system provides also the opportunity of following a specific temperature evolution. For instance, as reported in Fig. 8, it is possible to apply a constant heating rate (1200 K/min in these tests) and, after controlling the maximum temperature, impose a given cooling rate until a second temperature plateau is reached. This feature could be

really useful for semicrystalline thermoplastic materials, in which it is possible to control the development of the crystalline phase and morphology.

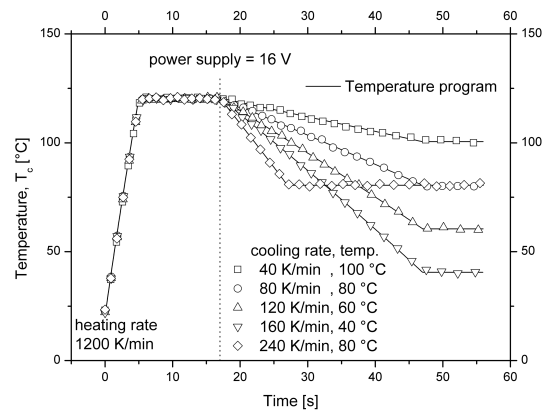


Fig. 8. Examples of possible controls of the thermal history. The power supply was 16 V. Just for these examples, the PES layer was 300 μm thick.

In order to check the homogeneity of the surface temperature, a thermographic analysis was carried out during a heating step with an infrared thermal camera, FLIR ThermoCAM, with 50 images per second. The results are reported in Fig. 9 and show that after about 5 s, namely when the maximum temperature is reached, the system presents a homogeneous surface temperature.

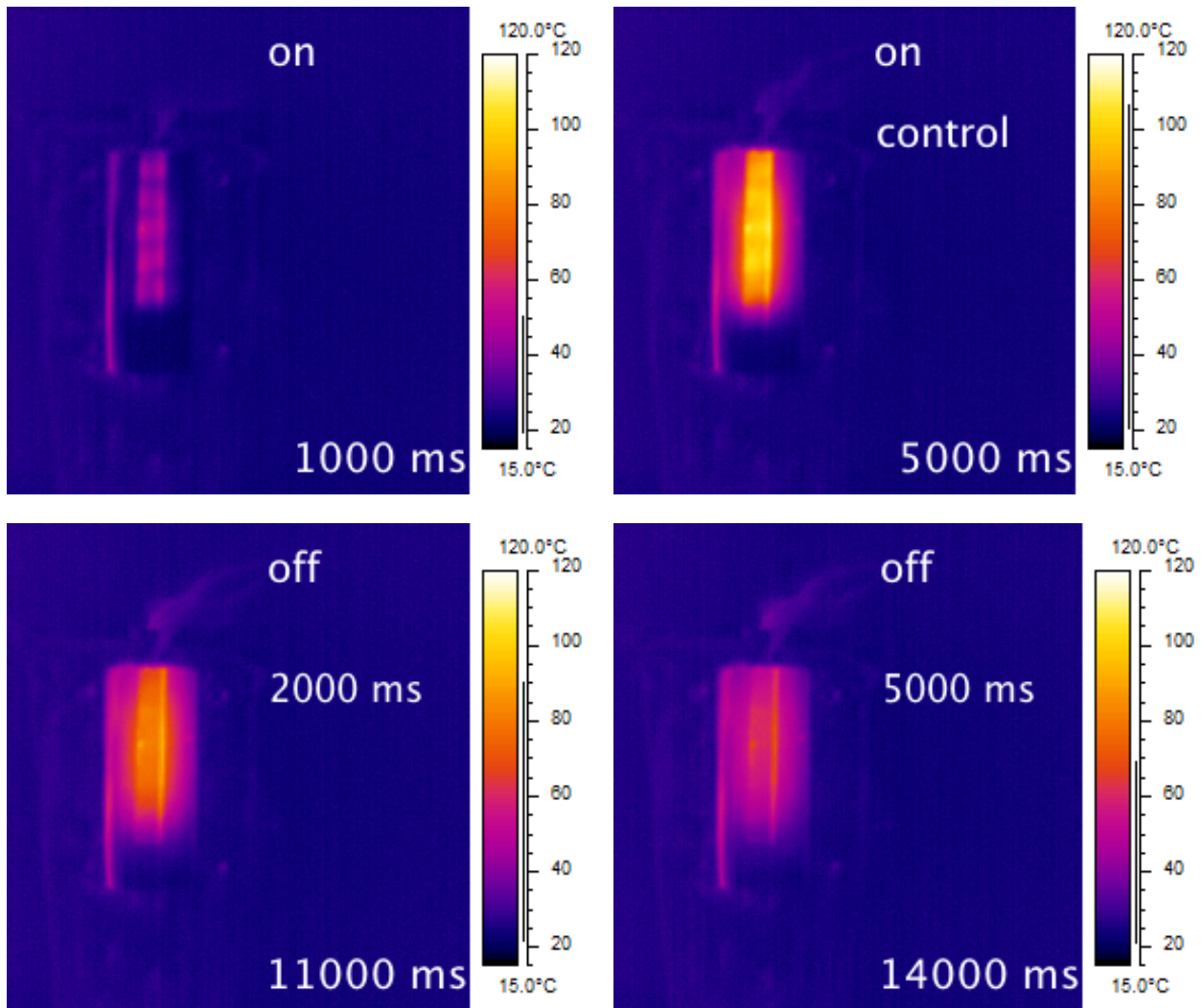


Fig. 9. Thermographic analysis after 1 s of heating, 5 s of heating, 2 s after switching off, 5 s after switching off. The power supply was 16 V.

2.3. Material

The material adopted for the molding tests was a commercial isotactic polypropylene, iPP, supplied by Montell (now Basell), with the commercial name of T30G. The material characterization was reported in the literature, in particular: the rheological behavior (Sorrentino and Pantani, 2013), the flow induced crystallization (Pantani et al., 2014a; Pantani et al., 2014b), the modeling of morphology evolution in the injection molding process (Pantani et al., 2005), crystallization kinetics (De Santis and Pantani, 2013), and the effect of the flow on spherulitic growth and nucleation rates (De Santis et al., 2016).

2.4. Injection molding tests

Two series of molding tests were carried out by imposing an injection temperature of 230°C. Three injection pressures were adopted: 100 bar, 150 bar and 200 bar. The pressure was kept for 5 s. Two mold temperatures were applied: 70°C

and 120°C. The heating system was switched-on 5 s before injection and switched off at the pressure release. The cavity adopted for the molding tests was rectangular, 200 µm thick, 5 mm wide and 20 mm long. The sample weight, if the cavity is completely filled with polypropylene, is less than 20 mg. After demolding, the length of the samples was measured by a digital caliper in order to assess the flow length for each molding conditions.

2.5. Characterization of injection molding parts

Two of the samples were microtomed to obtain slices 60 µm thick according to the scheme reported in Fig. 10. In particular, we analyzed the samples molded with an injection pressure of 200 bar and the mold temperatures: 25°C and 120°C. The slices were cut at a distance of 3 mm from the gate and observed in polarized light adopting an Olympus microscope.

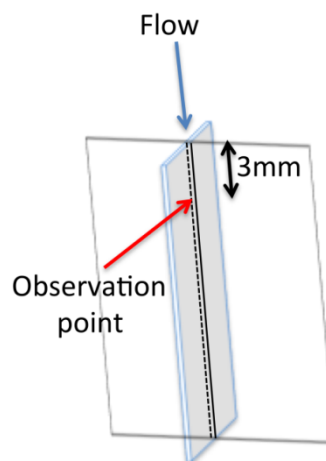


Fig. 10. Schematic of the cutting procedure and the observation position for the micrographs and the X-Ray analysis.

X-ray diffraction measurements (XRD) were performed with a Bruker D8 Advance diffractometer (equipped with a continuous scan attachment and a proportional counter) with Ni-filtered Cu K α radiation ($\lambda = 1.54050 \text{ \AA}$). The diffractograms were analyzed by a deconvolution procedure performed according to a scheme reported in the literature by Coccorullo et al. (Coccorullo et al., 2003).

The thermal mechanical properties of the samples were determined by dynamic mechanical analysis (DMA), using a PerkinElmer DMA8000 to determine the viscoelastic properties in the tension mode. Samples were heated from 40 °C to melting at a heating rate of 3 K/min at a frequency of 1 Hz.

3. Results and discussion

3.1. Flow length

The flow length reached for each molding tests is reported in Fig. 11 versus the imposed pressure for both the mold temperatures applied.

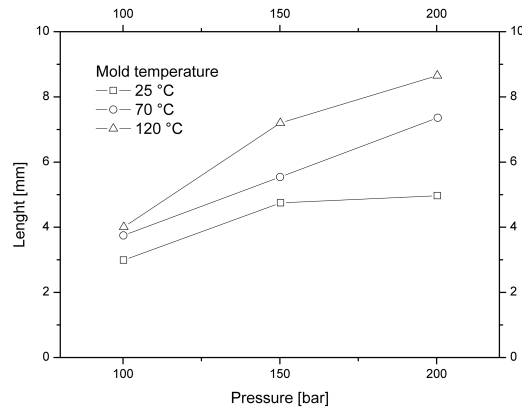


Fig. 11. Achieved flow length as a function of pressure for three mold temperatures.

The flow length increases on increasing pressure as normally found in spiral-flow tests. The effect of mold temperature is clear: on increasing the mold temperature the flow length increases so that for the highest applied pressure and mold temperature it was possible to fill nearly half of the cavity; vice versa, without the heating system, the flow length was shorter than 5 mm for all the applied pressures. Preliminary tests were conducted, in which all the mold was at the temperature of 150 °C, and the cavity resulted completely filled. Actually it is not possible to reach the same temperature with heating system of the surface of the mold because of the resulting break down of the electrical resistance for the required voltage.

3.2. Optical microscopy

The micrographs of the microtomed slices are presented in Fig. 12. The differences in the morphology of the samples is quite evident. The sample molded with a high mold temperature (Fig. 12A and 12B) presents a spherulitic morphology in the whole cross-section. This is obviously due to the fact that the flow takes place under a high temperature, and the molecular orientation is kept low because of a low relaxation time. After filling, the polymer has the time to crystallize during cooling essentially in quiescent conditions.

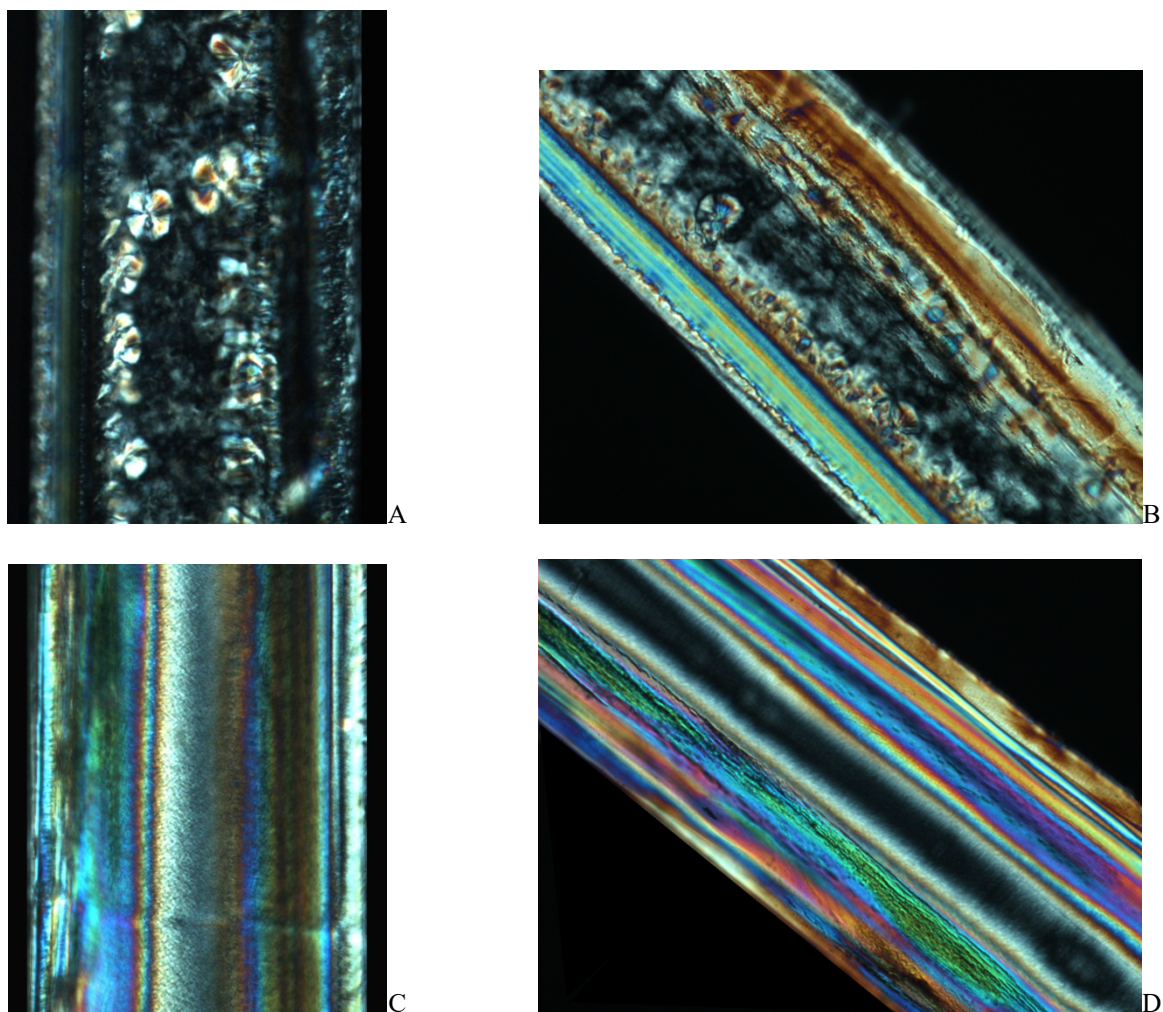


Fig. 12. Microtomed slices of molded samples in polarized light. The thickness of the samples is 200 μm . The holding pressure is 200 bar. A: mold surface 120°C. B: same sample as in A, after a 45° rotation; C: mold surface 25°C, D: same sample as in C, after a 45° rotation.

The distribution of spherulite dimensions (which appear to be smaller on reducing the distance from the mold surface) is due to both differences in cooling rate and to an enhanced nucleation rate induced by flow at position closer to the mold walls. Some bright β spherulites are also clearly visible. The β phase of polypropylene is normally not obtained under standard processing conditions since it is overcome by the α phase (Varga, 2002). However, under high shearing rates, this crystalline phase can form and grows faster than α phase for temperatures in the range of 100°C–140°C

(Zhang et al., 2011). This explains the presence of large β spherulites in the samples molded with a surface temperature of 120°C.

The morphology of the sample molded with a low surface temperature is completely different (Fig. 12C and 12D). In particular, no spherulitic morphology is detectable, even close to the midplane. The layer closer to the surface present a very oriented structure due to flow taking place at low temperature.

Fig. 13 shows the comparison of color fringe patterns between the samples molded with 200 bar of holding pressure and mold surfaces at 25°C and 120°C. Pictures have been taken by placing the samples in crossed polarized light. The sample molded with the lowest surface temperature presents clear fringes, especially at positions closer to the tips, indicating high orientation levels. Vice versa, the sample molded with the highest surface temperature is quite homogeneous in color, indicating a low birefringence in the whole part. The homogeneity of the sample is the most interesting result for any technological application.

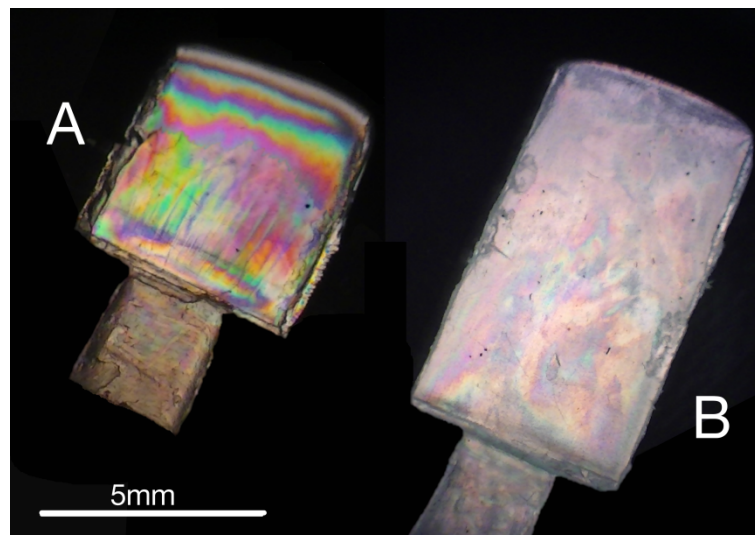


Fig. 13. Fringe patterns in polarized optical light for the samples molded with 200 bar of holding pressure. A: mold surface 25°C. B: mold surface 120°C.

3.3. X-Ray analysis

The X-Ray spectra of the samples molded with a surface temperature of 25°C and 120°C are reported in Figs. 14A and 14B, respectively. The peaks of the α phase of iPP, described by the Miller's indices (hkl) with corresponding Bragg angle 2θ : (110) by 14.5°, (040) by 17.2°, (130) by 19°, (111) by 21.5°, and (041) by 22.3°, are all present. It can be noticed for both samples the presence of a peak of the β phase of iPP corresponding to the plane (030) at $2\theta=16.1^\circ$. This peak is more evident for the sample molded with a surface temperature of 120°C, due to the fact that at in that temperature range the crystallization kinetics of β form presents a maximum.

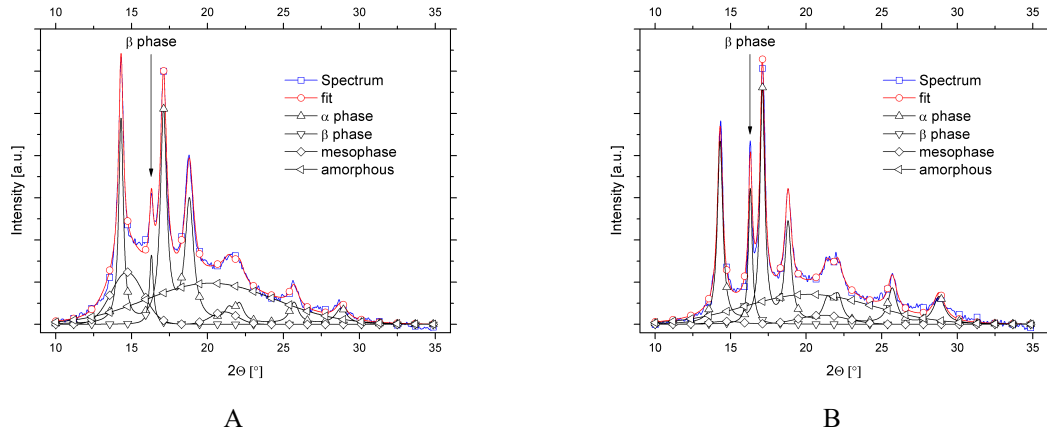


Fig. 14. WAXD analysis of the samples. A: mold surface 25°C. B: mold surface 120°C. The deconvolution of each crystalline peak is also reported.

The deconvolution procedure revealed that both samples present the same amount of amorphous phase, however the amount of mesomorphic phase (which is known to develop at high cooling rates (Coccorullo et al., 2003; De Santis et al., 2006, 2007) is much higher for the sample molded with the lowest surface temperature, as reported in Table 2.

Table 2. Percentage of the crystalline and amorphous phases inside the samples according to WAXD devonvolution.

Phase	Surface temperature	
	25°C	120°C
α	43.2%	52.2%
β	2.9%	7.2%
Mesomorphic	14.8%	4.9%
Amorphous	39.1%	35.7%

From the relative intensities of the peaks in the WAXD spectra it is possible to quantify the orientation levels according to the method introduced by Trotignon and Verdu (Trotignon et al., 1982). This method is based on the fact that the intensity of the peaks at $2\theta=21.5^\circ$ and 22.31° corresponding to the Miller's indices (111) and (041), respectively, reduce on increasing the orientation of the crystals. Two orientation indices can thus be calculated

$$A_{110} = \frac{I_{110}}{I_{110} + I_{111} + I_{131} + I_{041}} \quad (6)$$

$$A_{130} = \frac{I_{130}}{I_{110} + I_{111} + I_{131} + I_{041}} \quad (7)$$

where I_{hkl} represents the intensity at maximum diffraction for a defined (hkl) crystallographic plane. The calculated values for A_{110} and A_{130} are reported in Table 3. These indices stress the much lower orientation level present in the sample molded by adopting a higher surface temperature.

Table 3. Orientation indices as calculated by Eqs. (6) and (7).

Orientation index	Surface temperature	
	25°C	120°C
A_{110}	0.87	0.79
A_{130}	0.81	0.68

3.4. DMA analysis

The mechanical properties of polymeric samples are determined by the morphology. The results of DMA analysis is reported in Fig. 15.

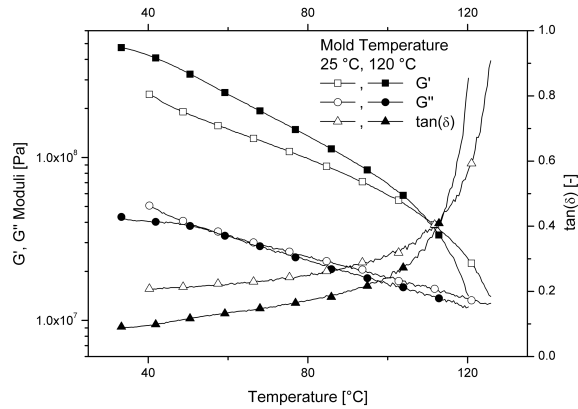


Fig. 15. DMA analysis of the samples. A: mold surface 25°C. B: mold surface 120°C.

The sample molded with the highest surface temperature shows a larger elastic modulus G' , but a lower resistance to temperature. The higher G' can be justified by the larger amount of α phase, which makes the sample more rigid during cantilever testing. The sample molded with the lowest surface temperature is instead characterized by a larger amount presence of mesomorphic phase, resulting in a lower elastic modulus.

The highest resistance to temperature can be instead justified by the oriented crystalline structures, which are present in much larger amount for the sample molded with the lowest surface temperature, and could have a larger melting temperature.

4. Conclusions

In this work, a system for rapid surface heating was designed, built and applied to a cavity for micro-injection molding. The system resulted to be able to increase the mold surface temperature of some tenths of Celsius degrees in a time of the order of one second. The system was applied to a particular mold, developed on purpose, which allows an easy change of geometry, surface materials and even thickness of each element that compose the mold itself. This feature could be really useful for semicrystalline thermoplastic materials, in which it is possible to control the development of the crystalline phase and morphology. Injection molding tests were then carried out by using an isotactic polypropylene and a cavity 200 μm thick. The effect of mold temperature on the flow length was as expected dramatic: it was possible to double the length of the part in the narrow rectangular channel in which without heating the flow length was few millimeters in the same pressure conditions. The morphology of the samples was assessed by means of polarized optical microscopy. The samples molded with a high mold temperature presented a spherulitic morphology in the whole cross-section. In the samples molded with a low surface temperature the spherulitic morphology was detectable only at the positions close to the midplane whereas the layer closer to the surface present a very oriented structure due to flow taking place at low temperature. Both optical microscopy and WAXD revealed the presence of a significant amount of β phase in the sample molded with a high surface temperature. The different morphology induced by a different mold surface resulted in a different mechanical behavior testified by DMA analysis. In particular, the sample molded with the highest surface temperature resulted to have a larger modulus (due to the larger amount of α phase) and a lower resistance to temperature (due to a lower molecular orientation).

Acknowledgments

The authors wish to thank Antonio Iannaccone, Ricardo Sora and Giovanni Marmora for carrying out some of the experiments during their project works for thesis. The support of prof. G. Cuccurullo from the Department of Industrial Engineering of the University of Salerno is also acknowledged as far as the thermographic analysis is concerned.

References

- Berger, G., Pacher, G., Pichler, A., Friesenbichler, W., Gruber, D., 2014. Influence of mold surface temperature on polymer part warpage in rapid heat cycle molding, PROCEEDINGS OF PPS-29: The 29th International Conference of the Polymer Processing Society-Conference Papers. AIP Publishing, pp. 189-194.
- Coccorullo, I., Pantani, R., Titomanlio, G., 2003. Crystallization kinetics and solidified structure in iPP under high cooling rates. *Polymer* 44, 307-318. Pii S0032-3861(02)00762-0
Doi 10.1016/S0032-3861(02)00762-0
- De Santis, F., Adamovsky, S., Titomanlio, G., Schick, C., 2006. Scanning Nanocalorimetry at High Cooling Rate of Isotactic Polypropylene. *Macromolecules* 39, 2562-2567. 10.1021/ma052525n
- De Santis, F., Adamovsky, S., Titomanlio, G., Schick, C., 2007. Isothermal nanocalorimetry of isotactic polypropylene. *Macromolecules* 40, 9026-9031
- De Santis, F., Pantani, R., 2013. Nucleation density and growth rate of polypropylene measured by calorimetric experiments. *Journal of thermal analysis and calorimetry* 112, 1481-1488
- De Santis, F., Pantani, R., Titomanlio, G., 2016. Effect of shear flow on spherulitic growth and nucleation rates of polypropylene. *Polymer* 90, 102-110
- Giboz, J., Copponnex, T., Mélé, P., 2007. Microinjection molding of thermoplastic polymers: a review. *Journal of micromechanics and microengineering* 17, R96. <http://dx.doi.org/10.1088/0960-1317/17/6/R02>
- Jansen, K., Flaman, A., 1994. Construction of fast-response heating elements for injection molding applications. *Polymer Engineering & Science* 34, 894-897. <http://dx.doi.org/10.1002/pen.760341105>
- Liparoti, S., Sorrentino, A., Guzman, G., Cakmak, M., Titomanlio, G., 2015. Fast mold surface temperature evolution: relevance of asymmetric surface heating for morphology of iPP molded samples. *RSC Advances* 5, 36434-36448
- Lucchetta, G., Fiorotto, M., Bariani, P.F., 2012. Influence of rapid mold temperature variation on surface topography replication and appearance of injection-molded parts. *Cirp Ann-Manuf Techn* 61, 539-542. 10.1016/j.cirp.2012.03.091
- Meister, S., Seefried, A., Drummer, D., 2015. Replication quality of micro structures in injection moulded thin wall parts using rapid tooling moulds. *Microsystem Technologies*, 1-12
- Pantani, R., Coccorullo, I., Speranza, V., Titomanlio, G., 2005. Modeling of morphology evolution in the injection molding process of thermoplastic polymers. *Prog Polym Sci* 30, 1185-1222. 10.1016/j.progpolymsci.2005.09.001
- Pantani, R., Nappo, V., De Santis, F., Titomanlio, G., 2014a. Fibrillar Morphology in Shear-Induced Crystallization of Polypropylene. *Macromolecular Materials and Engineering* 299, 1465-1473

- Pantani, R., Speranza, V., Titomanlio, G., 2014b. Evolution of iPP Relaxation Spectrum during Crystallization. *Macromolecular Theory and Simulations* 23, 300-306. <http://dx.doi.org/10.1002/mats.201300147>
- Sha, B., Dimov, S., Griffiths, C., Paekianather, M.S., 2007. Investigation of micro-injection moulding: Factors affecting the replication quality. *J Mater Process Tech* 183, 284-296. 10.1016/j.jmatprotec.2006.10.019
- Song, M.C., Liu, Z., Wang, M.J., Yu, T.M., Zhao, D.Y., 2007. Research on effects of injection process parameters on the molding process for ultra-thin wall plastic parts. *J Mater Process Tech* 187, 668-671. 10.1016/j.jmatprotec.2006.11.103
- Sorrentino, A., Pantani, R., 2013. Determination of the effect of pressure on viscosity of an isotactic polypropylene. *Polymer bulletin* 70, 2005-2014. <http://dx.doi.org/10.1007/s00289-013-0913-4>
- Trotignon, J.P., Lebrun, J.L., Verdu, J., 1982. Crystalline polymorphism and orientation in injection-molded polypropylene. *Plast. Rubber Process. Appl.* 2, 247-251
- Varga, J., 2002. β -Modification of Isotactic Polypropylene: Preparation, Structure, Processing, Properties, and Application. *Journal of Macromolecular Science, Part B* 41, 1121-1171. 10.1081/mb-120013089
- Wang, G., Zhao, G., Guan, Y., 2013. Thermal response of an electric heating rapid heat cycle molding mold and its effect on surface appearance and tensile strength of the molded part. *Journal of Applied Polymer Science* 128, 1339-1352. <http://dx.doi.org/10.1002/app.38274>
- Whiteside, B., Martyn, M., Coates, P., Greenway, G., Allen, P., Hornsby, P., 2004. Micromoulding: process measurements, product morphology and properties. *Plastics, rubber and composites* 33, 11-17. <http://dx.doi.org/10.1179/146580104225018346>
- Yao, D.G., Chen, S.C., Kim, B.H., 2008. Rapid Thermal Cycling of Injection Molds: An Overview on Technical Approaches and Applications. *Adv Polym Tech* 27, 233-255. 10.1002/adv.20136
- Zhang, J., Guo, C., Wu, X., Liu, F., Qian, X., 2011. Effects of Processing Parameters on Flow-Induced Crystallization of iPP in Microinjection Molding. *Journal of Macromolecular Science, Part B* 50, 2227-2241. <http://dx.doi.org/10.1080/00222348.2011.562839>
- Zhao, G., Wang, G., Guan, Y., Li, H., 2011. Research and application of a new rapid heat cycle molding with electric heating and coolant cooling to improve the surface quality of large LCD TV panels. *Polymers for Advanced Technologies* 22, 476-487. <http://dx.doi.org/10.1002/pat.1536>